

Photopatterned Polymer Brushes Promoting Cell Adhesion Gradients

Bradley P. Harris,[†] Jaishankar K. Kutty,[‡] Edward W. Fritz,[‡] Charles K. Webb,[‡]
Karen J. L. Burg,[‡] and Andrew T. Metters^{*,†,‡}

*Department of Chemical and Biomolecular Engineering and Department of Bioengineering,
Clemson University, Clemson, South Carolina 29634*

Received December 16, 2005. In Final Form: March 8, 2006

The ability to spatially control cellular adhesion in a continuous manner on a biocompatible substrate is an important factor in designing new biomaterials for use in wound healing and tissue engineering applications. In this work, a novel method of engineering cell-adhesive RGD-ligand density gradients to control specific cell adhesion across a substrate is presented. Polymer brushes exhibiting spatially defined gradients in chain density are created and subsequently functionalized with RGD to create ligand density gradients capable of inducing cell adhesion on an otherwise weakly adhesive substrate. Cell studies indicate that these ligand-functionalized surfaces are noncytotoxic, with cellular adhesion increasing with RGD-ligand density across the gradient brush surface.

Introduction

The interactions between integrin receptors of mammalian cells and extracellular matrix (ECM) proteins regulate a wide array of cellular behavior, including adhesion, motility, and differentiation.^{1–5} In many cases, the active regions of these ECM proteins comprise short peptide sequences that can be fabricated into surface-attached ligands to study specific concentration-dependent cell–peptide interactions. The arginine-glycine-aspartic acid (RGD) peptide sequence, found within many ECM proteins, has been the most extensively studied of these motifs, and substrates presenting this peptide have found widespread use in adhesion research.⁶ Current efforts to precisely engineer cell adhesive or nonadhesive biomaterial surfaces focus on tailoring nonspecific polymer–cell interactions, surface adsorption of proteins, or covalent modification of self-assembled monolayers (SAMs).^{6–10} Clinical application of these techniques is limited because they can be difficult to regulate, have limited compatibility with biomaterial substrates, do not have the structural stability to survive in vivo, or present difficulties in preparing patterns of multiple ligands. For example, nonspecific polymer–cell interactions often induce a foreign body response in vivo that can lead to inflammation, thrombosis, aseptic loosening, local tissue waste, and implant encapsulation.¹⁰

Current attempts to establish specific interactions between cells and biomaterial surfaces rely upon the controlled adsorption of ECM adhesion proteins such as fibronectin.^{10–12} Changes in cell density and morphology have been related to the density of

fibronectin adsorbed on a surface. Several groups have shown that the amount of surface-adsorbed fibronectin can be controlled by the grafting density and molecular weight of inert polymer brushes.¹¹ However, because of the noncovalent nature of the protein–polymer interaction, the stability of these modified surfaces is limited. Furthermore, proteins such as fibronectin contain a wide array of chemical domains and biological ligands that may trigger a number of unwanted cellular responses when adsorbed to a synthetic substrate.

An alternative approach to directing cell adhesion involves the immobilization of adhesive cues through the selective covalent functionalization of a nonadherent polymer brush with cell-adhesive ligands. The flexible chains of a multifunctional polymer brush, as well as the ability to modify the surfaces of both inorganic and polymeric materials, give this technique significant advantages compared to ligand immobilization on self-assembled monolayers (SAMs). Typically, SAMs are formed on inorganic substrates such as gold, silicon, or metal oxides. It is difficult to translate the orientational order achieved during self-assembly to the polymeric scaffolds used in many tissue engineering applications. Furthermore, compared to a polymer brush, SAM surfaces are fairly rigid because of their short chain lengths and densely packed structure. Because cell adhesion depends not only on integrin receptor occupancy but also on receptor clustering, the ability of a cell to cluster RGD units present on SAM surfaces may be limited as compared to the ability to cluster those attached to a flexible polymer brush.^{7,10}

This letter presents a novel method of creating RGD-ligand density gradients from anionic polymer brushes to control the spatial attachment of fibroblasts across patterned surfaces. Of particular interest is the ability to engineer gradient surfaces that present biological cues directing cell growth, adhesion, or movement. By utilizing a controlled photopolymerization technique developed previously, position-dependent thickness gradients of surface-attached polymer chains are created such that the grafting density varies continuously along the length of the gradient while the molecular weight of the attached polymer chains remains essentially constant.¹³ The control over chain density provided by this method is needed to fabricate such devices

* To whom correspondence should be addressed. E-mail: metters@clemson.edu.

[†] Department of Chemical and Biomolecular Engineering.

[‡] Department of Bioengineering.

(1) Hynes, R. O. *Cell* **1992**, *69*, 11–25.

(2) Clark, E. A.; Brugge, J. S. *Science* **1995**, *268*, 233–239.

(3) Schwartz, M. A.; Schaller, M. D.; Ginsberg, M. H. *Annu. Rev. Cell Dev. Biol.* **1999**, *11*, 549–599.

(4) Schwartz, M. A. *J. Cell Biol.* **1997**, *139*, 575–578.

(5) Streuli, C. H.; Bissell, M. J. *J. Cell Biol.* **1990**, *111*, 1405–1415.

(6) Houseman, B. T.; Mrksich, M. *Biomaterials* **2001**, *22*, 943–955.

(7) Maheshwari, G.; Brown, G.; Lauffenburger, D. A.; Wells, A.; Griffith, L. G. *J. Cell Sci.* **2000**, *113*, 1677–1686.

(8) Reznia, A.; Healy, K. E. *J. Biomed. Mater. Res.* **2000**, *52*, 595–600.

(9) Dillmore, W. S.; Yousaf, M. N.; Mrksich, M. *Langmuir* **2004**, *20*, 7223–7231.

(10) Hersel, U.; Dahmen, C.; Kessler, H. *Biomaterials* **2003**, *24*, 4385–4415.

(11) Bhat, R. R.; Tomlinson, M. R.; Genzer, J. J. *Polym. Sci., Part B: Polym. Phys.* **2005**, *43*, 3384–3394.

(12) Picart, C.; Elkaim, R.; Richert, L.; Audoin, F.; Arntz, Y.; Da Silva Cardoso, M.; Schaaf, P.; Voegel, J.-C.; Frisch, B. *Adv. Funct. Mater.* **2005**, *15*, 83–94.

(13) Harris, B. P.; Metters, A. T. *Macromolecules*, published online Jan 13, <http://dx.doi.org/10.1021/ma0512051>.

because it has been shown that the grafting density of the surface-attached polymer plays an important role in cell attachment and spreading.¹¹ Furthermore, by grafting monomers of defined functionality, modification of the resulting substrate-bound polymer chains can be carried out using well-characterized chemistries to attach bioactive ligands to the polymer brush. It is hypothesized that this versatile functionalization scheme can be used to generate areal gradients in ligand density across substrate surfaces. Because the cellular response to substrate-bound adhesion molecules is well characterized,¹⁴ it is further hypothesized that creating surfaces with increasing concentrations of cell adhesion ligands will facilitate the ability to control cell adhesion and motility spatially and temporally across various biomaterials for use in wound healing therapies such as chronic ulceration and nerve regeneration where well-choreographed cell responses are requisite.

Experimental Section

Polymerization. A derivatized photoiniferter, *N,N*-(diethyl-aminodithiocarbamoylbenzyl(tri-methoxy)silane) (SBDC) was synthesized as described previously.¹⁵ A self-assembled monolayer (SAM) of SBDC was deposited on piranha-treated silicon wafers by standard monolayer deposition techniques. Silicon wafers were chosen for this study so that robust surface characterization techniques such as variable-angle ellipsometry could be used to fully characterize surface topography and ligand density in a manner not readily feasible on thick polymeric biomaterial scaffolds. Once the kinetics and conjugation behavior of these ligand-functionalized polymer brush systems have been elucidated, this technique should translate well to relevant biomaterial surfaces where certain surface analysis techniques cannot be performed.

Methacrylic acid (MAA, Aldrich, 99%) was used as a functional monomer for polymerization. A solution of MAA in deionized Milli-Q water was prepared and transferred to a reaction vessel containing a pretreated silicon wafer. The reaction vessel was covered with a glass plate and sealed under nitrogen. Sample irradiation for preparing the surface-bound macromolecular gradients was carried out by utilizing a custom-made device that varied exposure time across the surface while maintaining a constant intensity of 365 nm wavelength light.¹³ After polymerization, any physisorbed monomeric and polymeric MAA was removed by sonication for 2 to 3 h in ethanol (Aldrich, 99.8%).

Functionalization of Surface-Attached PMAA with RGD. The functionalization of gradient PMAA films with RGD (GRGDS, Bachem), a cell-adhesion peptide, utilized well-known carbodiimide chemistry to activate the carboxylic acid groups of PMAA.¹⁶ The conjugation reaction was conducted in two steps. In the first step, freshly made PMAA gradient films were immersed overnight in a solution of dicyclohexyl carbodiimide (DCC, Aldrich, 99%) and *N*-hydroxysuccinimide (NHS, Aldrich, 98%) with anhydrous tetrahydrofuran (THF, Aldrich, 99.9%) as the solvent. The absence of water from the first step, along with the addition of NHS to stabilize the reactive intermediate prior to conjugation, reduced hydrolysis and improved conjugation efficiency as compared to conducting the conjugation in an aqueous environment (data not shown). At the completion of the first step, the activated films were washed with copious amounts of water and ethanol to remove both the solvent (THF) and any byproducts of the reaction. Immediately following the washing step, the films were immersed in a pH 7.4 phosphate-buffered saline (PBS) solution containing RGD and allowed to react 12–16 h at room temperature. Finally, the functionalized surfaces were washed and sonicated in deionized Milli-Q water to remove unreacted RGD.

The dry layer thickness of the surface-attached polymer was measured both before and after functionalization with RGD using a Beaglehole Instruments phase-modulated picometer ellipsometer equipped with a photoelastic birefringence modulator. The ellipsometric angles as a function of the incident angle were fit using a Cauchy model (Igor Pro. software package) to determine the graft-layer thickness.^{13,17}

The RGD surface density, σ (molecules/nm²), was estimated for RGD-functionalized surfaces by the following equation¹⁸

$$\sigma = \frac{\rho h_d N_A^{-21}}{M} = \frac{602.3 \rho h_d}{M} \quad (1)$$

where ρ (g/cm³) is the bulk density of the attached macromolecule, h_d is the dry layer thickness (nm), N_A is Avogadro's number, and M (g/mol) is the molar mass of the attached molecule. Equation 1 was also used to calculate the conjugation efficiency (CE) of RGD to the PMAA polymer brush. In this case, the surface density of the RGD was compared to the surface density of the –COOH groups of PMAA at the same position along the gradient, as shown in eq 2:

$$CE = \frac{\frac{602.3 \rho_{\text{RGD}} h_{\text{RGD}}}{M_{\text{RGD}}}}{\frac{602.3 \rho_{\text{PMAA}} h_{\text{PMAA}}}{M_{\text{PMAA}}}} \times 100\% = \frac{\rho_{\text{RGD}} h_{\text{RGD}} M_{\text{PMAA}}}{\rho_{\text{PMAA}} h_{\text{PMAA}} M_{\text{RGD}}} \times 100\% \quad (2)$$

Here, ρ_{RGD} is the density of RGD, ρ_{PMAA} is the bulk density of the PMAA brush, h_{RGD} is the thickness change upon functionalization with RGD, h_{PMAA} is the dry layer thickness of the PMAA brush (minus the thickness of the initial SBDC SAM layer), M_{RGD} is the molecular weight of RGD, and M_{PMAA} is the molecular weight of PMAA.

Cell Culture Studies. Clonetics 3T3 mouse fibroblast cells were used to assess cell adhesion and spreading across the functionalized gradient and control surfaces. The cells were cultured in Dulbecco's modified Eagle's medium (DMEM-F12 50:50, Fisher Scientific) supplemented with 10% (v/v) fetal bovine serum at pH 7.4. Approximately 2×10^4 3T3 mouse fibroblast cells were seeded per 1 cm² specimen and incubated in a 7.5% CO₂ atmosphere at 37 °C. For quantification of cell densities on sample and control surfaces, cells were fixed after 24 h with 4% paraformaldehyde for 40 min and then permeabilized with 0.1% Triton-x. Prior to fixation and analysis, samples were washed twice with phosphate-buffered saline (50 mM, pH 7.4) to remove unattached cells. The surface-attached cells were then stained with 4'-6-diamidino-2-phenylindole (DAPI; Molecular Probes) and imaged at 4× magnification. Statistical analysis was performed using a one-tailed student's t-test. To assess cell viability and long-term cell adhesion, additional samples and controls were cultured for up to 1 week. Optical microscopy (100× magnification) was used to image representative areas of these gradient and control surfaces throughout the course of the experiment. After 5 days of incubation, cell viability was assessed via a live/dead viability assay from Molecular Probes (L-3224).

Results and Discussion

Formation and Functionalization of PMAA Surfaces with RGD. In the case of surface-initiated photopolymerization, because of high graft densities, the polymer chains adopt an upright and stretched “brush” configuration.^{13,17} As shown in previous studies, the gradient-exposure system used in the current work produces gradients in the grafted-chain density but not the polymer molecular weight across the substrate surface because of the lack of dithiocarbamyl groups available for reversible

(14) Wong, J. Y.; Velasco, A.; Rajagopalan, P.; Pham, Q. *Langmuir* **2003**, *19*, 1908–1913.

(15) de Boer, B.; Simon, H. K.; Werts, M. P. L.; van der Vegte, E. W.; Hadziioannou, G. *Macromolecules* **2000**, *33*, 349–356.

(16) Kurzer, F.; Zadeh-Douraghi, K. *Chem. Rev.* **1967**, *67*, 107–152.

(17) Rahane, S. B.; Kilbey II, S. M.; Metters, A. T. *Macromolecules* **2005**, *38*, 8202–8210.

(18) Liu, Y.; Klep, V.; Zdyrko, B.; Luzinov, I. *Langmuir* **2004**, *20*, 6710–6718.

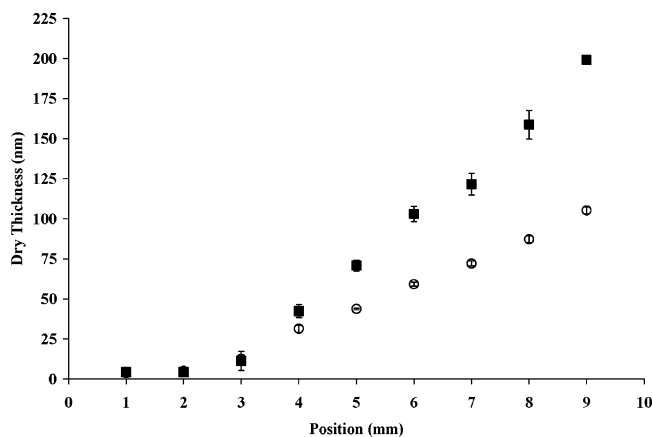


Figure 1. Ellipsometric dry layer thickness vs position for surface-attached PMAA (O) and RGD-functionalized PMAA (PMAA-RGD) (■). Exposure conditions: [MAA] = 50% v/v in DI water; incident light intensity (365 nm) = 10 mW/cm²; mask rate: 12 mm/h.

termination.^{13,17} Without these moieties to reversibly terminate the growing chain ends, the rate of propagation is much higher than initiation, and uncontrolled free-radical polymerization takes place.¹⁹ The rate at which polymer is deposited on the surface is therefore determined by the time-dependent initiation of the surface-tethered photoiniters. A grafting density gradient is produced by increasing the fraction of activated photoiniters with exposure time. This produces a unilateral increase in the brush-layer thickness across the surface.¹³ In Figure 1, a continuous molecular-thickness gradient of PMAA was formed on a single silicon wafer by linearly increasing UV exposure time with position along a single axis of the substrate.

Because PMAA possesses side-group carboxylic acid functionalities, an amidation reaction was conducted to functionalize the polymer chains with ligands containing primary amines. After functionalization, the polymer chains stretch to greater thicknesses than seen with unfunctionalized chains because of greater steric interactions. As shown in Figure 1, upon functionalization with RGD, the dry layer thickness of the functionalized polymer is significantly greater than that of the unfunctionalized PMAA. The thickness change upon conjugation is directly related to the amount of RGD ligand immobilized on and within the surface-tethered polymer layer via the reactive carboxylic acid groups. Furthermore, the greater slope of the thickness plot of the PMAA-RGD polymer gradient compared to the original PMAA film indicates increasing ligand density with position.

In Figure 2, both the RGD surface density and the conjugation efficiency are plotted as functions of the unconjugated dry layer thickness. Using the thickness data from Figure 1, the RGD ligand density was calculated from eq 1, and the conjugation efficiency was calculated using eq 2. As shown in Figure 2, the RGD density increases across the gradient surface as the dry layer thickness increases, indicating the presence of an RGD-ligand density gradient across the surface. Furthermore, using the above conjugation scheme, the obtained RGD densities within the grafted surface layer are several orders of magnitude higher than those typically achieved with conventional peptide surface-attachment methods.⁸ It is important to note, however, that the ligand densities shown in Figure 2 represent the entire modified PMAA layer. In its dry state, this layer is up to 200 nm thick and will swell upon exposure to the cell culture media. However, on the basis of current literature, it is thought that only the upper

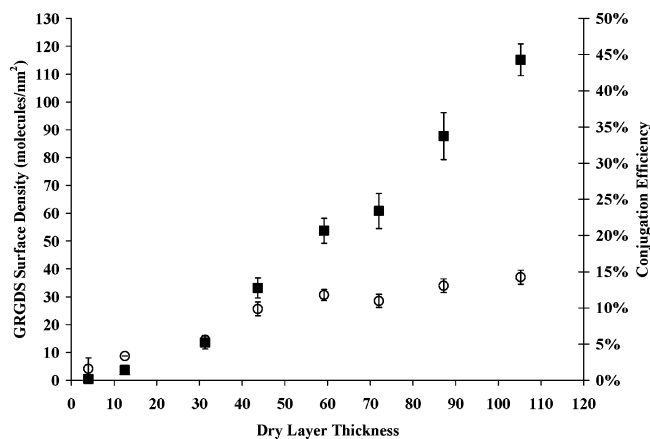


Figure 2. RGD surface density (■) and overall conjugation efficiency (O) for RGD-functionalized PMAA films.

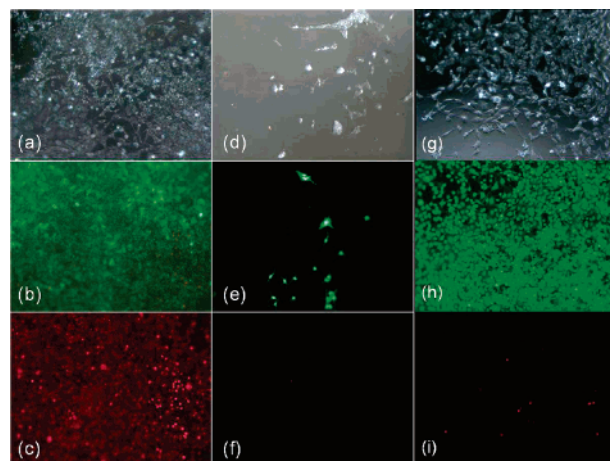


Figure 3. Day 5 cell culture images of control surfaces. (a) 100× bright-field image of an SBDC-SAM surface, dry layer thickness (T) = 1.6 nm; (b) live cells on SBDC-SAM stained with a 4 μ M calcein AM solution; (c) dead cells on SBDC-SAM stained with a 4 μ M ethidium homodimer-1 solution; (d) 100× bright-field image of an unconjugated PMAA surface, T = 100 nm; (e) live cells on unconjugated PMAA stained with a 4 μ M calcein AM solution; (f) dead cells on SBDC-SAM stained with a 4 μ M ethidium homodimer-1 solution; (g) 100× bright-field image of a PMAA-RGD conjugated surface, T = 200 nm, RGD surface density of approximately 100 molecules/nm²; (h) live cells on PMAA-RGD stained with a 4 μ M calcein AM solution; (i) dead cells on PMAA-RGD stained with a 4 μ M ethidium homodimer-1 solution.

5 to 10 nm of the film will be accessible to the cells and as such only RGD surface densities in this region will be critical for adhesion.^{10,20} Assuming a uniformly conjugated layer, the calculated RGD surface concentrations for the upper 10 nm of the gradient layer presented in Figure 1 range from 80 pmol/cm² to 8.3 nmol/cm². These values are still much higher than the femtomolar surface concentrations reported using techniques such as adsorption, modified SAM layers, and covalent hydrogel derivatives.^{10,20}

Conjugation efficiency data presented in Figure 2 indicates that a maximum of 12 ± 2% of the pendant PMAA acid groups are successfully conjugated using the described two-step process. Furthermore, on the basis of Figure 2, conjugation efficiency increases up to a dry layer thickness of approximately 40 nm, after which it remains essentially constant. It is thought that the conjugation efficiencies of the thicker PMAA films are limited by large grafted-chain densities that minimize the mass transfer

(19) Odian, G. In *Principles of Polymerization*, 4th ed.; Wiley-Interscience: Hoboken, NJ, 2004; pp 198–350.

(20) Elbert, D. L.; Hubbell, J. A. *Biomacromolecules* **2001**, *2*, 430–441.

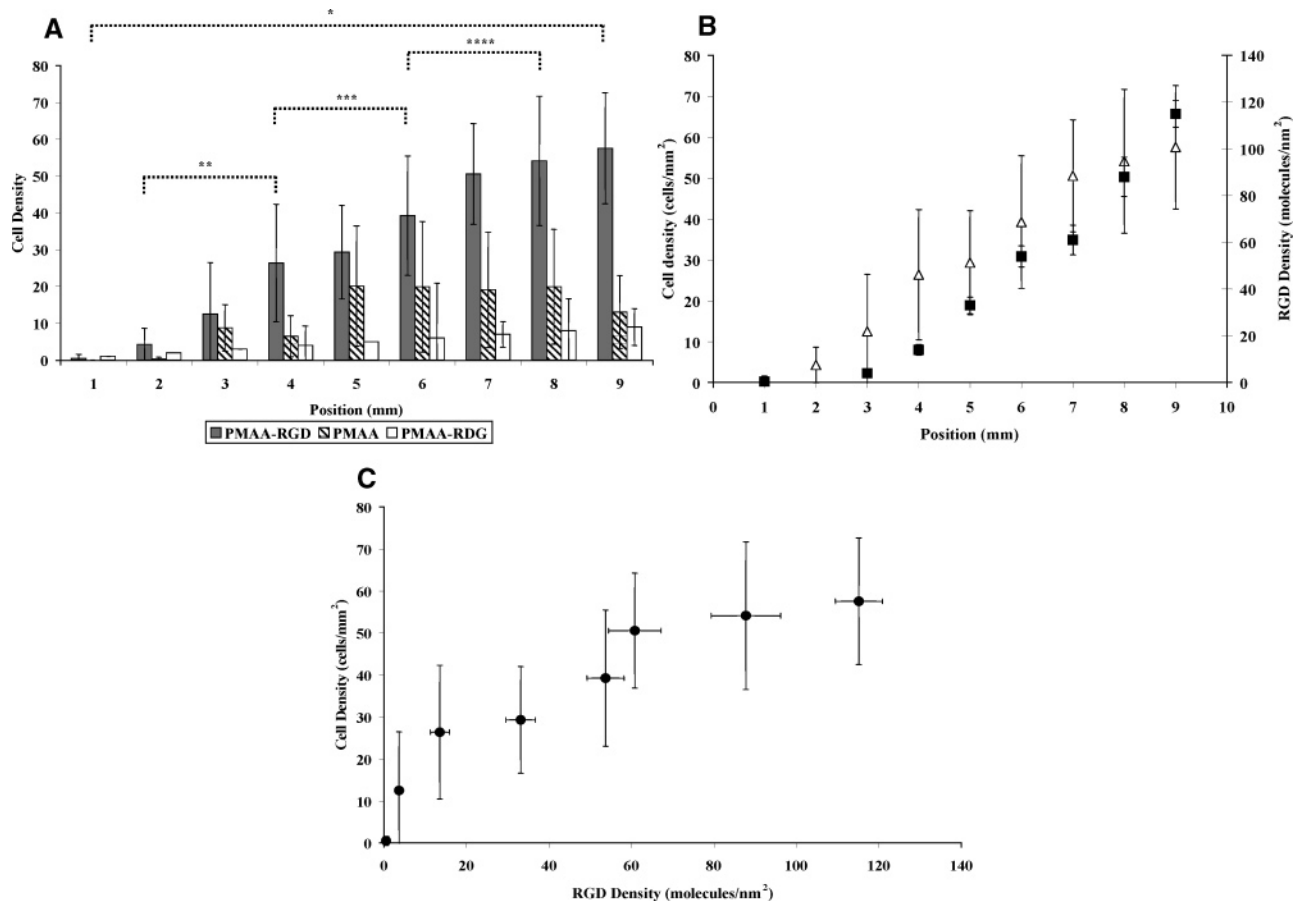


Figure 4. (A) Average cell density vs position for PMAA–RGD, PMAA–RDG, and unmodified PMAA surfaces. PMAA brush layer thickness increases with position in a similar manner for all samples (Figure 1). Average cell density and standard deviations were calculated at each position from a series of eight pictures taken perpendicular to the gradient across two samples. Cell densities on the PMAA–RGD surfaces compared at each position shown were different with the following levels of significance: (*) $p < 0.0005$, (**) $p < 0.0005$, (***) $p < 0.025$, and (****) $p < 0.01$. At all positions except 1 and 3 mm, cell densities on PMAA–RGD surfaces were significantly higher than those observed on PMAA–RDG ($p < 0.001$) or unmodified PMAA surfaces ($p < 0.05$). (B) Cell density (Δ) and RGD density (■) vs position for the PMAA–RGD-functionalized films. (C) Cell density vs RGD density for the PMAA–RGD-functionalized films.

of RGD into the polymer brushes. Nevertheless, results presented in Figure 2 indicate the creation of an RGD–ligand density gradient across the substrate.

Influence of RGD Ligand Density Gradients on Cellular Adhesion. The use of polyelectrolytic PMAA brushes is especially beneficial for isolating the cell-specific interactions of RGD peptides because the anionic nature of PMAA brushes effectively repels most nonspecific cell adhesion.²¹ To make the PMAA surfaces significantly cell-adhesive, bioactive ligands must be reacted into the polymer brush. By selective functionalization of the polymer brush using the straightforward procedure described above, gradients in RGD ligand density across an otherwise anionic PMAA surface should facilitate specific cell adhesion to the surface in regions of high RGD density while being notably less cell-adhesive in regions of low RGD density. However, because a maximum of 12% of the anionic brush is functionalized during the conjugation process, many acidic groups remain in the PMAA–RGD layer after functionalization. It is hypothesized that the anionic charge density underlying the PMAA–RGD layer (through unconjugated acid groups) will influence the strength of cell attachment to the RGD surface through long-range interactions and facilitate the need for higher RGD surface densities compared to previous studies.

In Figure 3, cell culture images of both control and RGD-functionalized surfaces are shown. The SBDC–SAM surface prior to polymerization with MAA is cell-adhesive (Figure 3a). However, it is also highly cytotoxic, with large numbers of dead cells present as indicated by a live/dead viability assay (Figure 3b and c). Upon grafting PMAA brushes to the SBDC–SAM substrate, the modified surface becomes non-cell-adhesive and noncytotoxic as indicated by Figure 3d–f.

The minimally adhesive character of the PMAA brushes was maintained for over 1 week in cell culture with serum proteins present. This observed cell repellency is quite different than what is observed with –COOH end-functionalized SAM layers where significant protein adsorption and cell adhesion have been observed.²² The nonadhesive character of PMAA brushes is most likely due to the dramatically higher concentration of carboxylic acid groups at the surface resulting in a significant anionic charge and reduction in pH near the surface.

Upon functionalization of the nonadhesive PMAA brushes (Figures 3d–f) with RGD, the substrate becomes cell-adhesive and noncytotoxic (Figures 3g–i). Contact-angle measurements show no change in the wettability of the surfaces with increasing RGD concentration. Furthermore, the functionalization of PMAA brushes with the nonintegrin binding sequence GRDGS shows

(21) Higashi, J.; Nakayama, Y.; Marchant, R. E.; Matsuda, T. *Langmuir* **1999**, *15*, 2080–2088.

(22) Fauchoux, N.; Schweiss, R.; Lutzow, K.; Werner, C.; Groth, T. *Biomaterials* **2004**, *25*, 2721–2730.

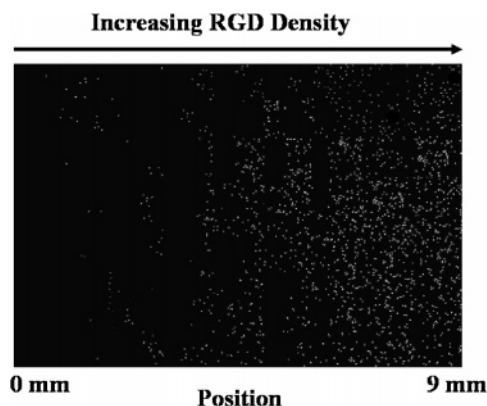


Figure 5. Twenty-four hour cell culture image of a PMAA-RGD modified film. The image is a compilation of 72 individual images taken at $4\times$ magnification across the RGD-functionalized surface. The cell nuclei were stained with DAPI for cell counting and appear as small white dots on the black background. Cell number and density increase from left to right as RGD-ligand density increases. (Quantitative results are shown in Figure 4B.)

minimal cell adhesion (Figure 4A), confirming that cell adhesion on RGD-functionalized surfaces is based on specific, integrin-mediated binding and not on nonspecific hydrophobic or ionic interactions. Thus, by grafting PMAA chains to the cytotoxic, cell-adhesive SBDC-SAM surface, the resulting substrate becomes weakly adhesive and noncytotoxic. Subsequent functionalization of the PMAA chains with the RGD adhesion ligand readily transforms the surface from weakly adhesive to strongly cell-adhesive in a single facile step while maintaining biocompatibility.

In Figure 4, the quantitative cell adhesion results obtained on PMAA-RGD, PMAA-RDG, and unmodified PMAA gradient substrates are examined at different points along the gradient. The comparison provided by Figure 4A shows that cell density across the PMAA-RGD-functionalized surfaces increases with position parallel to the ligand gradient and is significantly higher than the corresponding cell adhesion on either PMAA-RDG or unmodified PMAA surfaces. Figure 4B demonstrates the collinear increase in both cell density and RGD density with position for PMAA-RGD gradient films. Cell density statistically increases with RGD density in regions with ligand densities of less than $60 \text{ molecules/nm}^2$ (Figure 4A and B, positions 1–7 mm). However, from Figure 4C, it appears that at RGD surface densities above approximately $60 \text{ molecules/nm}^2$ a saturation effect occurs at which further increases in RGD surface density do not improve cell adhesion.

Finally, Figure 5 presents a compiled microscopy image of cells adhering in a gradient fashion across the entire PMAA-RGD film 24 h after uniform seeding. As RGD density increases across the grafted layer, cell adhesiveness markedly increases from relatively few adherent cells at low surface density to a nearly confluent layer at high surface density. This supports the hypothesis that ligand-mediated binding is the predominant cell-material interaction occurring on the PMAA-RGD surfaces. The results of live/dead viability assays on identical RGD-functionalized surfaces also indicate that this surface is highly cytocompatible and nontoxic, with very few dead cells present (Figure 3g–i).

Conclusions

The creation of surfaces exhibiting position-dependent chain density gradients of a functional anionic monomer has been described. Unlike the behavior of $-\text{COOH}$ -functionalized SAM surfaces presented in the literature,²² these acidic gradient brushes were resistant to cell adhesion presumably because of the highly concentrated anionic nature of the brush. These surfaces were then functionalized with cell-adhesive RGD ligands to create materials exhibiting ligand density gradients that influenced specific cell adhesion in a spatially defined manner across a macroscopic substrate. The functionalized materials were shown to be cytocompatible and cell-adhesive. Furthermore, cell adhesion was shown to preferentially increase in the direction of increasing RGD density until a limiting RGD density was reached (approximately $60 \text{ molecules/nm}^2$).

It is hypothesized that presenting RGD to cellular receptors using functionalized polymer brushes will enhance cell adhesion and cell recognition of the binding motif as compared to other methods of ligand immobilization. Because the number of attached cells is related to the RGD surface density and high ligand densities should lead to increased focal adhesion formation,¹⁰ the strength of cellular attachment on ligand-functionalized polymer brushes should be greater than on SAMs or adsorbed fibronectin because of the dramatically larger ligand densities achievable. Furthermore, the polymer chains of the functionalized gradient polymer brush should be more flexible than those of oligomeric, tightly packed SAMs. The increased mobility of the brush layer will lead to increased focal-adhesion formation and improved strength of attachment because integrin-mediated cell adhesion depends on receptor clustering^{7,10} and the cells' improved ability to rearrange a flexible polymer chain so as to obtain maximum receptor clustering for binding.

Therefore, by using the method outlined in this work to prepare a gradient polymer brush with cell-adhesive ligands, the ability to control the type and degree of specific cell-material interactions across a synthetic surface is readily achievable. This is advantageous for applications requiring spatially and biochemically specific cellular responses such as in vivo nerve regeneration and wound healing. Furthermore, the simplicity of creating either a nonadhesive anionic polymer brush or an adhesive directed-response system with the above techniques should allow for rapid incorporation into existing biomaterial scaffolds. For example, several previous reports in the literature discuss the modification of polymeric substrates using a structurally similar photoiniferter.^{21,23–26} Finally, the methods presented in this work also open the door to high-throughput cell-biomaterial analysis.

Acknowledgment. The authors are grateful to ORAU and NSF for financial support of this research through a Ralph E. Powe award to A.T.M. and a PECASE award (BES 0093805) to K.J.L.B. Surface characterization was also made possible with assistance from the NSF-sponsored Center for Advanced Engineering of Fibers and Films (award no. EEC-9731680).

LA053417X

(23) Luo, N.; Hutchinson, J. B.; Anseth, K. S.; Bowman, C. N. *Macromolecules* **2002**, *35*, 2487–2493.

(24) Luo, N.; Hutchinson, J. B.; Anseth, K. S.; Bowman, C. N. *J. Polym. Sci., Part A: Polym. Chem.* **2002**, *40*, 1885–1891.

(25) Luo, N.; Metters, A. T.; Hutchinson, J. B.; Bowman, C. N.; Anseth, K. S. *Macromolecules* **2003**, *36*, 6739–6745.

(26) Nakayama, Y.; Matsuda, T. *Macromolecules* **1996**, *29*, 8622–8630.